BIOCHEMISTRY
including biophysical chemistry & molecular biology

Article

pubs.acs.org/biochemistry

Simulation of Catalytic Water Activation in Mitochondrial F_1-ATPase Using a Hybrid Quantum Mechanics/Molecular Mechanics Approach: An Alternative Role for β-Glu 188

Fernando Martín-García,[†,‡] Jesús I. Mendieta-Moreno,[†,‡] Íñigo Marcos-Alcalde,[†] Paulino Gómez-Puertas,*[,†] and Jesús Mendieta[†,‡]

[†]Molecular Modelling Group, Centro de Biología Molecular "Severo Ochoa" (CSIC-UAM), C/Nicolás Cabrera, 1, Cantoblanco, 28049 Madrid, Spain

[‡]Biomol-Informatics, Parque Científico de Madrid, C/Faraday, 7, Cantoblanco, 28049 Madrid, Spain

Supporting Information

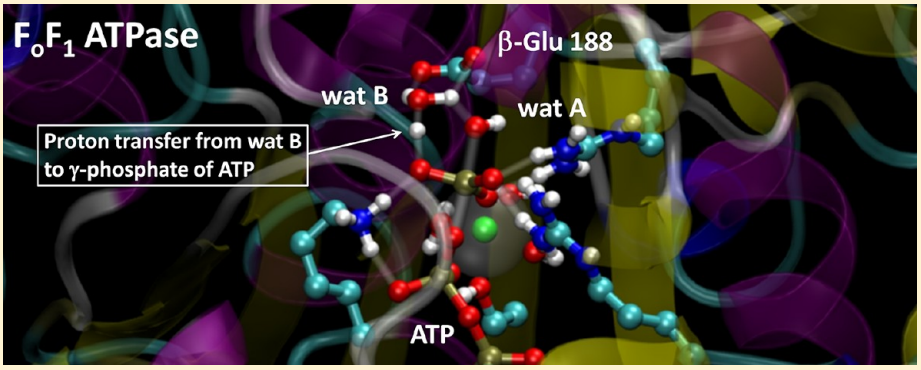

ABSTRACT: The use of quantum mechanics/molecular mechanics simulations to study the free energy landscape of the water activation at the catalytic site of mitochondrial F_1-ATPase affords us insight into the generation of the nucleophile OH^- prior to ATP hydrolysis. As a result, the ATP molecule was found to be the final proton acceptor. In the simulated pathway, the transfer of a proton to the nucleotide was not direct but occurred via a second water molecule in a manner similar to the Grotthuss mechanism proposed for proton diffusion. Residue β-Glu 188, previously described as the putative catalytic base, was found to be involved in the stabilization of a transient hydronium ion during water activation. Simulations in the absence of the carboxylate moiety of β-Glu 188 support this role.

Mitochondrial F_oF_1-ATP synthase is the enzyme responsible for the synthesis of ATP from ADP and P_i ($H_2PO_4^-$).[1,2] Unlike the majority of the enzymes, which work by increasing the rate of the reactions that they catalyze, F_oF_1-ATP synthase can force the reaction far from equilibrium by harnessing the proton gradient,[3] working as a nanomachine that operates as a mechanical/chemical energy transducer.[4] Therefore, although the hydrolysis of ATP to ADP and P_i is an exergonic process, because of the activity of F_oF_1-ATP synthase, the ATP:ADP/P_i concentration ratio is close to 1:1 in mitochondria.[5,6] The enzyme is able to generate this gradient even under conditions that favor the hydrolysis reaction by a factor of 2×10^5.[7]

The three-dimensional structure of F_oF_1-ATP synthase[8−12] presents two different substructures: a globular catalytic moiety (F_1) and a transmembrane portion (F_o) whose rotation is induced by the proton gradient. F_1-ATP synthase has three pairs of α and β subunits located around the γ subunit, which presents a globular head domain and an extended coiled-coil tail.[8] Both the α and β subunits are able to bind to nucleotides, but only β subunits are considered catalytically active. Most of the residues that stabilize ATP binding are located in the β subunit, with the catalytic site located at the interface between the α and β subunits. An α subunit closes the catalytic site on the triphosphate moiety. At least one residue from the α subunit (α-Arg 373) is hydrogen-bonded to an oxygen of the nucleotide.

It has been demonstrated that ATP synthesis depends on an external torque on the γ subunit, causing a clockwise rotation and successive structural modifications of the pairs of α and β subunits that result in the generation of ATP molecules from ADP and P_i.[13] During ATP hydrolysis, in contrast, the enzyme rotor turns counterclockwise also in a complex mechanism involving different conformations of the β subunits and consecutive steps of liberation of P_i, Mg^{2+}, and ADP after the hydrolysis event.[14]

Received: August 16, 2012
Revised: November 19, 2012
Published: January 15, 2013

dx.doi.org/10.1021/bi301109x | *Biochemistry* 2013, 52, 959−966

As a general mechanism, the first steps in the hydrolysis of triphosphate nucleotides require the activation of a water molecule.[15] The resulting OH^- group attacks the γ-phosphorus, weakens the bond between this atom and the bridging oxygen, and forces the atoms to adopt the trigonal bipyramidal geometry characteristic of the pentacovalent transition state.[16] When the attacking nucleophile has a relatively high pK_a, e.g., in the case of water, it is commonly assumed that the biological phosphoryl transfer reaction has to be catalyzed by a general base that initially accepts the proton from the nucleophile.[17] The identity of the general base in the different reactions has often been a question of interest and debate.

In the case of F_1-ATPase, the first ATP hydrolysis mechanism proposed was based on the crystal structure of the protein, determined in the presence of ADP and P_i by Abrahams et al.[8] In that structure, residue β-Glu 188 is hydrogen-bonded to the catalytic water in a position that makes it a strong candidate to act as the catalytic base. In the reverse reaction, during ATP synthesis, β-Glu 188 could provide the proton for the abstraction of the water molecule.[18] The ability of glutamic acid to act as the general base in ATP hydrolysis depends on its pK_a. In general, glutamic residues require a very hydrophobic environment to operate as efficient proton acceptors. Although a study predicted that the pK_a of a modified residue in the equivalent position in thermophilic F_1-ATPase could be particularly high,[19] in the polar environment of the active site of F_1-ATPase it is supposed that the pK_a of β-Glu 188 is low. Under these conditions, the pK_a of the ATP molecule makes it a much more favorable candidate general base.[20] This hypothesis, in which the nucleotide is involved in its own hydrolysis, has previously been proposed for ras p21[21] and named substrate-assisted catalysis.[22]

A favorable reaction path with ATP as the final proton acceptor has previously been proposed for F_1-ATPase using a theoretical approach.[23,24] The transfer of a proton to the ATP along that path involves two water molecules. However, the system used in the study was only a part of the total β subunits, and more than 50% of the atoms included in the study were fixed to preserve the overall shape of the system. More recently, protonation of β-Glu 188 involving three water molecules has been described assuming a different reaction path in a "dissociative" manner.[25] Experimental observations were provided in the same work showing that the rate-determining step of the reaction is the transfer of a proton from the catalytic water molecule. In similar systems, indirect proton transfer has also been proposed for myosin-catalyzed ATP hydrolysis.[26]

We have recently developed a quantum mechanics/molecular mechanics (QM/MM) approach to generate the free energy surface of the conformational space defined by the reaction coordinates for water activation in the GAP−ras p21 complex.[27] The results suggest that GTP can act as the catalytic base, with the proton being transferred from the attacking water molecule to the nucleotide along an indirect path involving a second water molecule, the most favorable pathway. In this work, we use a similar approach to study an F_1-ATPase QM/MM system that includes in the MM region the whole α and β subunits in a fully unconstrained simulation, in contrast to the previously published analysis, which includes in the MM only a small portion of the proteins around the active site.[23−25] The study of the energy surface could afford us insight into the residues involved in the activation of the catalytic water molecule in F_1-ATPase.

EXPERIMENTAL PROCEDURES

Molecular Dynamics (MD) Simulations. The system used in our simulations was based on the X-ray structure determined by Menz et al.[12] [Protein Data Bank (PDB) entry 1H8E]. The system includes the F and B chains corresponding to the β and α subunits. Aluminum fluoride and ADP molecules included in the crystal structure so that it resembles the structure of the transition state were replaced with an ATP residue with transition state geometry. The distance between the oxygen of the catalytic water molecule (HOH numbered as F2128 in PDB entry 1H8E) and the P_γ atom of the ATP was held at 1.9 Å by an imposed restraint. The distance between the P_γ atom of the ATP and the bridging oxygen interacting with the P_β atom was also restrained to 1.9 Å. A second water molecule (HOH F2130) was also included in the simulated system.

The system was immersed in a rectangular parallelepiped solvent box, and a distance of 12 Å was maintained between the wall of the box and the closest atom of the solute. K^+ ions were added to neutralize the negative charge, with the counterions placed in a shell around the protein moiety using a Coulomb potential in a grid. The counterions and the solvent were added using the LEaP module of AMBER.[28] All the MD simulations were performed using the AMBER11 PMEMD program[28,29] and the parm99 parameter set.[28] Initial relaxation of the system was achieved by performing 10000 energy minimization steps using a cutoff of 10.0 Å. Subsequently, and to start the molecular dynamics (MD) simulations, the temperature was increased from 0 to 298 K in a 500 ps heating phase, and velocities were reassigned at each new temperature according to a Maxwell−Boltzmann distribution. During this period, the dihedrals of the C_α trace were restrained with a force constant of 500 kcal mol^{-1} rad^{-2}. For the last 200 ps of the equilibration phase of the MD, the force constant was reduced stepwise to 0. The SHAKE algorithm was used throughout to constrain all hydrogen bonds to their equilibrium values so that an integration time step of 2 fs could be employed. The list of nonbonded pairs was updated every 25 steps, and coordinates were saved every 2 ps. Periodic boundary conditions were applied, and electrostatic interactions were represented using the smooth particle mesh Ewald method with a grid spacing of ~1 Å. The length of the trajectories was 10 ns in all cases.

Quantum Mechanics/Molecular Mechanics (QM/MM) Simulations. The hybrid QM/MM approach is a suitable simulation method for studying processes in which chemical bonds are formed and broken, such as enzymatic reactions. The QM/MM simulations were performed using the sander module of AMBER11.[29] The method requires the partitioning of the system into two regions, QM and MM. Calculations involving the atoms belonging to the QM region were performed using the PM3 semiempirical Hamiltonian. The atoms in the system that are not part of the QM region (those in the MM region) were treated in a classical MM way. In our system, the QM region includes two water molecules involved in the catalysis, and the ATP atoms from the γ-phosphate group to the C5′−C4′ bond. It also includes the Mg^{2+} ion and all the oxygen atoms in its coordination sphere, including the hydroxyl group of Thr 163 from the β subunit and three coordinating water molecules. Side chains of the Glu 188, Lys 162, and Arg 189 residues of the β subunit and the side chain of Arg 373 belonging to the α subunit are also included. The QM region contains 83 atoms, including six link H atoms used to complete

dx.doi.org/10.1021/bi301109x | Biochemistry 2013, 52, 959−966

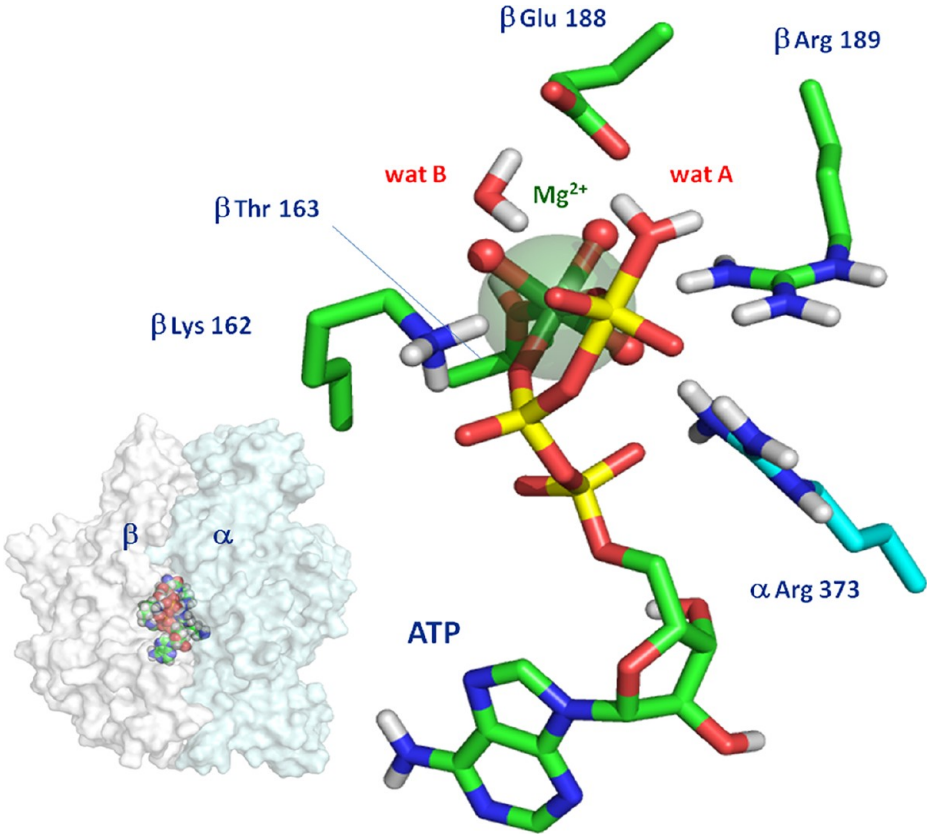

Figure 1. Schematic representation of the active center of F_1-ATPase. The ATP molecule was generated by superimposing the corresponding atoms of the F_1-ATPase structure on the original ADP and aluminum fluoride molecules (PDB entry 1H8E). ATP is associated with a Mg^{2+} atom (green sphere), which includes three water molecules in its coordination sphere (red spheres indicate the positions of the oxygen atoms of the water molecules). The positions of the catalytic water (wat A) and an additional water molecule (wat B) are indicated. Residues of the β subunit (Glu 188, Lys 162, and Arg 189) and the α subunit (Arg 373) located in the active center are also labeled. The inset shows a complete MD system, including whole α (white) and β (blue) subunits and showing the position of the atoms in the active center (spheres) at the interface between the two subunits after unconstrained MD simulation.

the covalent bonds cut by the QM/MM boundary.[28] The MM region includes all the other atoms described in the MD simulations (see above), including the whole α and β ATPase subunits. The conformation obtained after classical MD was then equilibrated again for 200 ps using this QM/MM approach. During the equilibration, the constraints corresponding to all the covalent bonds between the atoms in the QM region were maintained. All the restraints, except those corresponding to the parameters of the reaction and the position of the catalytic water, were progressively removed over the next 100 ps. SHAKE was not used for either the MM region or the QM region. A cutoff of 8 Å was used to calculate the QM/MM electrostatic interactions. The extra Gaussian terms that are used in the PM3 Hamiltonian to improve the core−core repulsion term in QM−QM interactions were also included for the QM−MM interactions.

Energy Surface Calculations. To explore the most important part of the conformational space defined by the reaction coordinates, a new approach was developed. The approach is based on adaptively biased MD[30] and presents some characteristics of steered MD[31] as well as an umbrella sampling[32] procedure. The O−H distance in the catalytic water (breaking distance) and the distance between the H of this catalytic water and the O of the second water molecule (bond distance) were used as the reaction coordinates in all the calculations. The QM/MM trajectories were performed by restraining both reaction coordinates using harmonic potentials with a flat bottom and parabolic sides. For each trajectory, the value of one coordinate was increased over the simulation time, as in steered MD,[31] from 0.95 to 2.0 Å, while the size of the flat bottom part of the harmonic potential of the other coordinate was kept constant within a narrow range. Overlapping of points between neighboring trajectories was observed, as in umbrella sampling procedures,[32] ensuring good coverage of the whole surface. The generation of a large number of trajectories makes it possible to explore the conformational space defined by the reaction coordinates in detail.

Using the hybrid QM/MM potential, the effective energy of the system can be divided into three components:

$$E_{\text{eff}} = \langle \Psi | H_{\text{QM}} + H_{\text{QM/MM}} | \Psi \rangle + E_{\text{MM}}$$

H_{QM} is evaluated using the chosen QM method (in our case, the PM3 Hamiltonian). E_{MM} is calculated classically from the MM atom positions using the AMBER force field equation and parameters. $H_{\text{QM/MM}}$ is the sum of an electrostatic term and a Lennard-Jones (van der Waals) term and represents the interactions between the atoms in the QM and MM regions. For our trajectories, E_{MM} was not taken into account because we consider that the H_{QM} and $H_{\text{QM/MM}}$ terms represent the influence of the protein moiety on the chemical reaction. We sampled the conformational space of the reaction at ~12000 homogeneously distributed points on a surface of 1.05 Å × 1.05

dx.doi.org/10.1021/bi301109x | *Biochemistry* 2013, 52, 959−966

Å. Three-dimensional smoothing of the data was applied using the local smoothing technique with tricube weighting and polynomial regression (LOESS).

RESULTS AND DISCUSSION

The starting configuration of the system used in this work includes the whole α and β subunits of the mitochondrial F_1-ATP synthase corresponding to the X-ray crystallographic structure determined by Menz et al.[12] (PDB entry 1H8E). The crystal structure contains ADP and aluminum fluoride to emulate the hydrolysis transition state. In our system, ADP and aluminum fluoride have been replaced by an ATP residue with transition state geometry. The residue was created by overlapping the corresponding portion with the ADP and superimposing the γ-phosphate on the Al atom. The minimal constraints necessary to maintain the geometry were applied to the distances and angles (see Experimental Procedures). Figure 1 shows the active site containing five water molecules: three of them are included in the coordination sphere of the Mg^{2+} ion. The other two water molecules are the catalytic one (wat A), which is involved in the generation of the transition state, and an additional water molecule (wat B) that is also located at the active site. After minimization and equilibration, a productive MD of 10 ns was performed. Figure 2A shows the root-mean-square deviation (rmsd) corresponding to the trace of the C_α atoms. During the simulation, the rmsd was almost constant at ~2 Å. This value, close to the resolution of the crystallized structure, shows that no significant conformational changes occurred during the adaptation of the system to the AMBER force field.

The behavior of wat A and wat B present in the active center was also monitored throughout the trajectory. Both of them are hydrogen bonded to β-Glu 188. Wat B also interacts through hydrogen bonding with an oxygen in the γ-phosphate. Figure 2B shows that the distances corresponding to these interactions remained constant during the simulation. The stability of the interaction between these water molecules and the residues of the active center suggests that both of them could be involved in the first steps of the reaction. Wat A and wat B were included in the QM region of the QM/MM system.

To study the nature of the catalytic base involved in ATP hydrolysis in F_1-ATPase, we used the hybrid QM/MM potential implemented in the AMBER11 package.[29] This approach presents some characteristics of steered MD and others of umbrella sampling procedures, and it is based on the adaptively biased MD method[30] to obtain a free energy surface of the conformational space defined by the reaction coordinates, as described previously.[27]

***β*-Glu 188 as the General Base.** Figure 3 shows the free energy landscape obtained for the activation of the catalytic water molecule assuming β-Glu 188 is the proton acceptor. The reaction parameters used in this case were the distance between the proton and the oxygen of the catalytic water and the distance between the proton and Oδ1 of the carboxylic group of β-Glu 188. The reaction proceeded through a high energy barrier (~28 kcal/mol) with the ΔG_0 value obtained for the protonation of the glutamate residue being ~25 kcal/mol. This value is compatible with a low pK_a characteristic of this acid residue in a polar environment. Both the high energy barrier and high ΔG_0 suggest that β-Glu 188 is not a good candidate to act as the general base. In general, glutamic acid residues require a very hydrophobic environment to work as proton acceptors, as under such conditions the electrostatic interactions are stronger than in polar environments and therefore the pK_a values become higher. The catalytic site of F_1-ATPase contains five negative charges (ATP^{4-} and β-Glu 188), five positive charges (β-Lys 162, β-Arg 189, α-Arg 373, and the Mg^{2+} ion), and five water molecules (wat A, wat B, and the three in the coordination sphere of the Mg^{2+} ion, which also includes β-Thr 163). In such a polar environment, β-Glu 188 must exhibit a low pK_a, which makes it difficult for this residue to act as a catalytic base. To provide further support to this statement, an additional simulation of proton transference between a Glu residue and an ATP molecule through a hydronium intermediate was performed in solution, simulating a polar environment (Figure S1 of the Supporting Information). As expected, the difference in ΔG_0 values of the system between the protonated states of the two molecules (4.5 kcal/mol), which corresponds to 3.3 pK_a units, is in the range of the experimentally measured difference of 3.0−3.3 pK_a units between the two groups in solution. This result indicated that our simulation approach is sufficiently accurate to capture the relative proton affinities of these two groups.

In the same free energy landscape (Figure 3), a second local minimum is observed in the top right-hand corner. The structure of the active center in this region shows a deprotonated β-Glu 188 residue and the pentacovalent

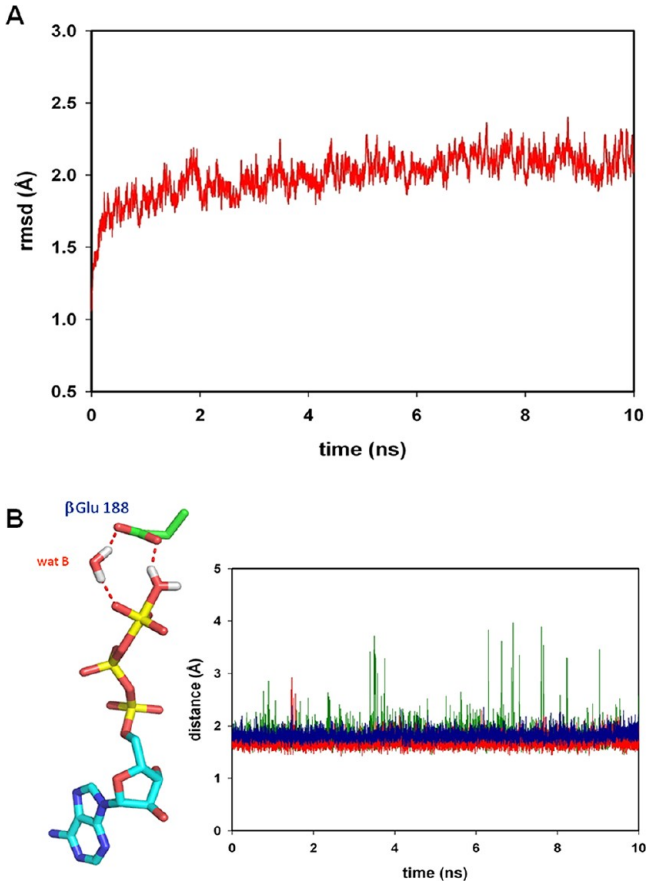

Figure 2. (A) Temporal profile of the C_α root-mean-square deviation (rmsd) of the whole system during unconstrained MD simulation. (B) Continuous measurement of the hydrogen bond distances between the protons of wat A and wat B and the oxygen atoms of β-Glu 188 (red and blue lines, respectively) as well as of the protons of wat B and the O3γ atom of the nucleotide (red line) during unconstrained MD simulation. Measured distances are graphically represented in the scheme on the left (dashed lines).

dx.doi.org/10.1021/bi301109x | *Biochemistry* 2013, 52, 959−966

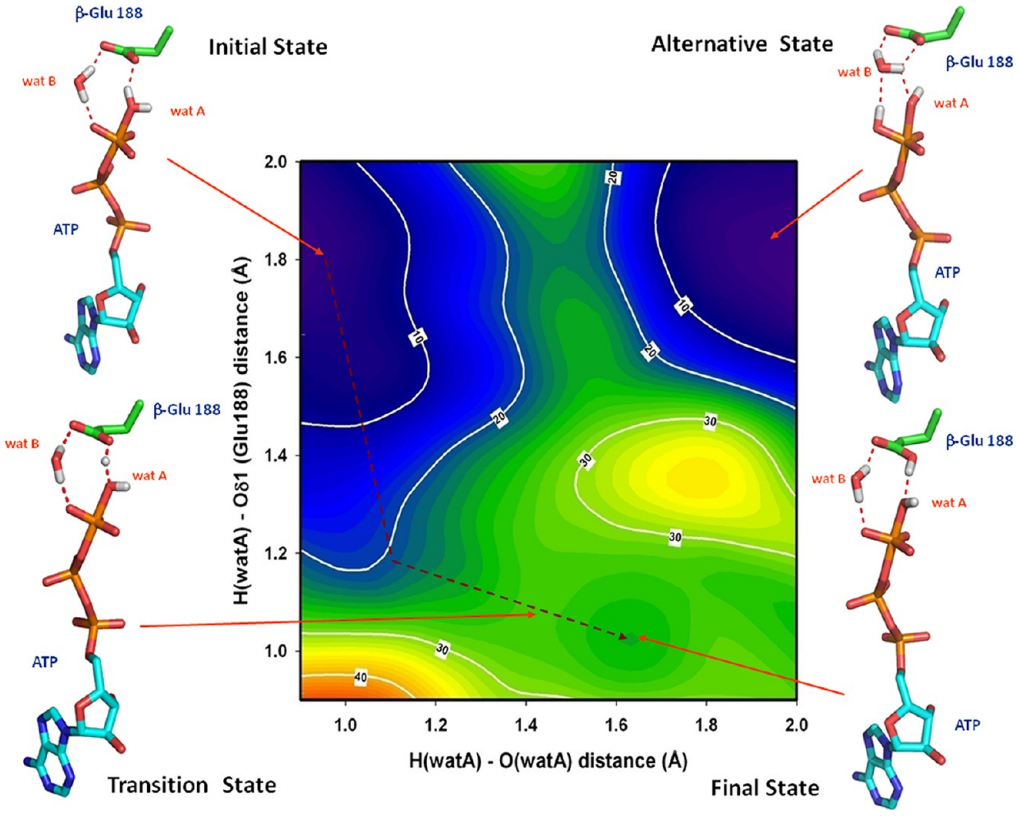

Figure 3. Free energy landscape for the activation of the catalytic water molecule assuming β-Glu 188 is the proton acceptor. ΔG_0 values obtained for the whole system are shown for the different states corresponding to the distances: x axis, from the proton to the oxygen atom in the active water molecule (wat A); y axis, from the same proton to Oδ1 of β-Glu 188. The structure of the active center is depicted in the initial, transition, and two alternative final states. In all cases, the γ-phosphate group of ATP exhibited a pentacovalent conformation.

transition state in a protonated form, suggesting that the final proton acceptor during the water activation could be the nucleotide. Interestingly, comparison of the structures in the initial and final states indicates that the original location of the proton bound to ATP in the final state was not the catalytic water molecule (wat A) but the second water molecule (wat B) present at the active site. This suggests a two-water mechanism, similar to that previously described for human Ras p21.[27]

ATP as the General Base. Figure 4 shows the free energy landscape obtained for the activation of the catalytic water molecule assuming ATP is the final proton acceptor instead of β-Glu 188. In this case, the reaction parameters were the distance between the proton and the oxygen of the catalytic water (wat A) and the distance between the proton and the oxygen of the second water molecule (wat B) present at the active site. Just as indicated above, the analysis of this trajectory indicated that the transfer of a proton from the catalytic water, wat A, to the nucleotide is not direct but occurs via the second water, in a manner similar to the Grotthuss mechanism proposed for proton diffusion,[33] as described for human Ras p21.[27]

The reaction proceeds through an energy barrier of ~22 kcal/mol, lower than the 28 kcal/mol value that corresponds to the barrier when β-Glu 188 was considered to be the proton acceptor (Figure 3). Significantly, the ΔG_0 value obtained for the final state of this reaction is close to 0 kcal/mol. The final structure shows a protonated pentacovalent transition state that is consistent with the high pK_a (~6.8) of ATP in polar environments.[20] This result suggests that the protonation of the ATP and the formation of the nucleophile OH^- ion from the catalytic water are more favorable than β-Glu 188 acting as a general base in the polar environment of the catalytic site.

To analyze the behavior of the protons in detail throughout the process, the reaction along the minimal energy path between the initial and final states was simulated (dashed line in Figure 4). Monitoring the proton movements (a video of the entire process is provided as Supporting Information) revealed that a proton from the catalytic water (wat A) is initially transferred to the additional water (wat B), thus forming a hydronium ion (H_3O^+). Then, a different proton from wat B is transferred to the ATP in the pentacovalent transition state. This behavior confirms a proton transfer path similar to the Grotthuss mechanism.[33]

The conformation of the catalytic site at the saddle point, corresponding to the transition state of the water activation (Figure 4), shows a strong interaction between the carboxylic group of β-Glu 188 and the hydronium ion formed when the additional water molecule (wat B) accepts the proton from the catalytic water molecule (wat A). This interaction stabilizes the transition state of the water activation, reducing the value of the energy barrier.

Noncarboxylate Moiety in the β-Glu 188 Position. The results obtained in the simulations described above suggest a new role for β-Glu 188, which is the stabilization of the hydronium ion generated transiently during the transfer of a proton from the catalytic water molecule to ATP. This important role could explain the lack of activity produced by mutations of this residue,[34−37] although it does not play a direct role as a catalytic base. It has been demonstrated that the presence of a carboxylate group at this position is definitely

dx.doi.org/10.1021/bi301109x | *Biochemistry* 2013, 52, 959−966

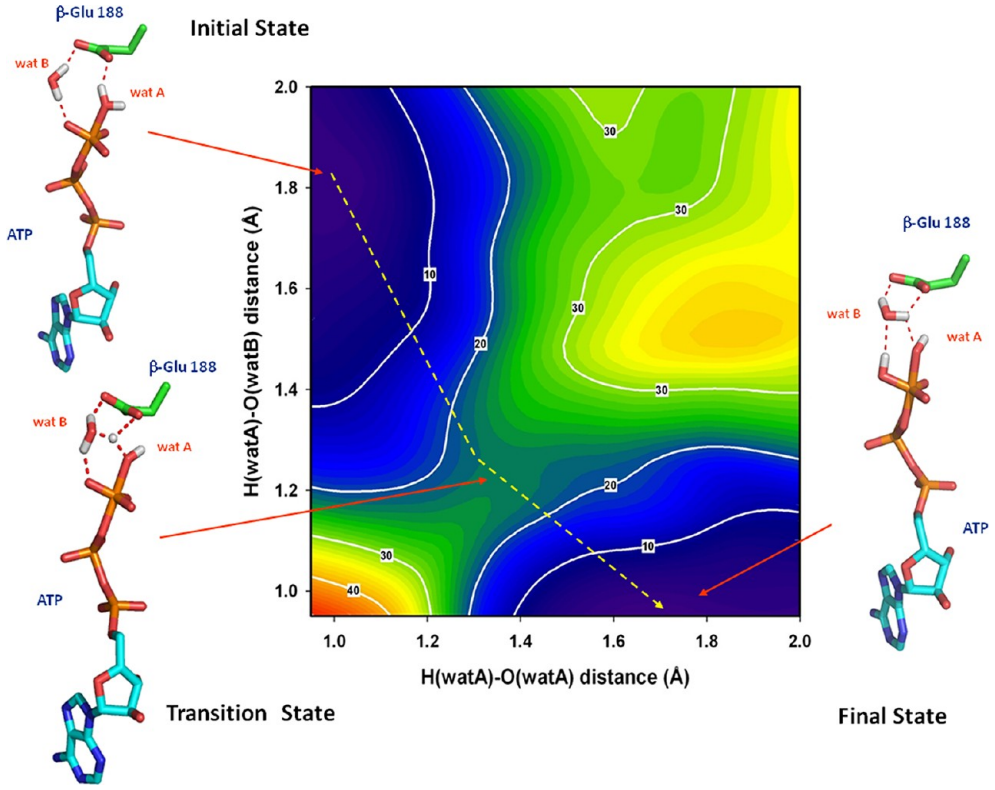

Figure 4. Free energy landscape for the proton transfer between the active water molecule (wat A) and the second water molecule (wat B). The axes represent the distances: *x* axis, from the proton to the oxygen atom in wat A; *y* axis, from the same proton to the oxygen atom in the second water molecule (wat B). *β*-Glu 188 stabilizes the position of the water molecules during proton transfer. The structure of the active center is depicted in the initial, transition, and final states. In the final state, a proton from wat B has been transferred to the ATP molecule.

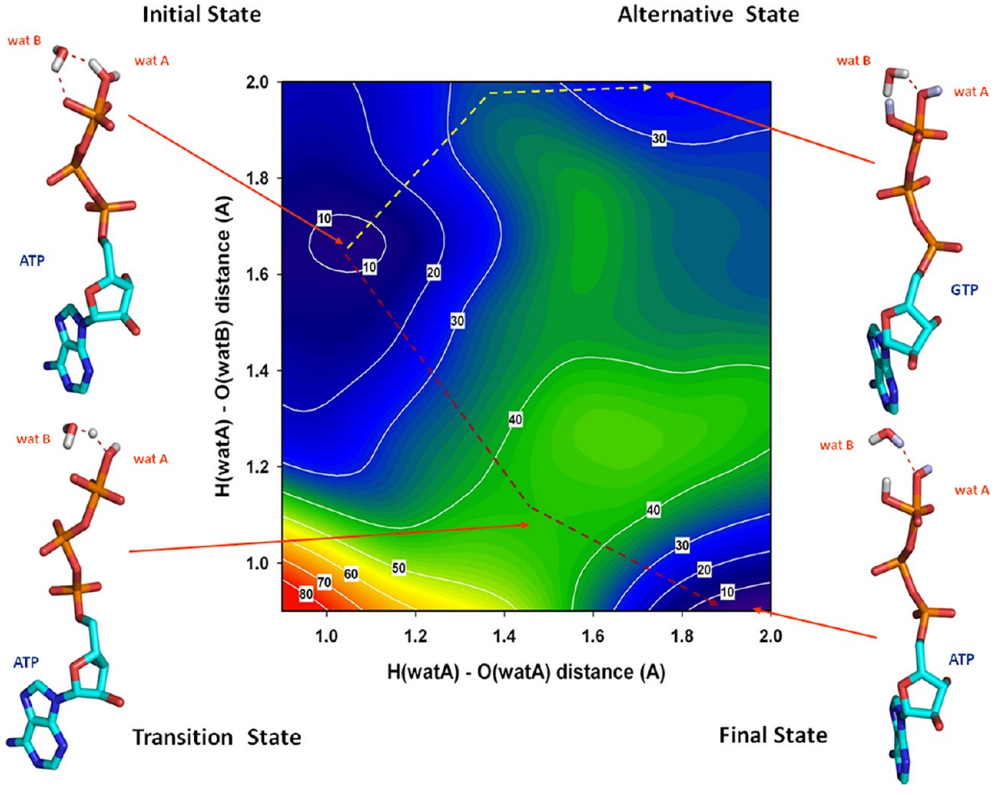

Figure 5. Free energy landscape in the absence of the carboxylate moiety in the *β*-Glu 188 position. Axes are defined as in Figure 4. The structure of the active center is depicted in the initial, transition, and final states. An alternative final state, located in an additional ΔG_0 minimum (top right), is also represented.

dx.doi.org/10.1021/bi301109x | *Biochemistry* 2013, 52, 959−966

required for catalysis and its spatial positioning needs to be very precise: only when β-Glu 188 is replaced by residues containing a carboxylate group (Asp or *S*-carboxymethylcysteine) is a small but detectable degree of ATPase activity retained by the enzyme.[36] Nevertheless, and to gain additional support for this hypothesis, we generated the free energy landscape for the same proton transfer path but simulating an inactive configuration in which the carboxylate moiety has been removed and the original Glu residue substituted with a neutral one (Ala). Figure 5 shows that the water activation in the absence of the carboxylic group of β-Glu 188 proceeds through a very high energy barrier of ∼42 kcal/mol, with the ΔG_0 value for the final state being close to 0 kcal/mol as in the case of the wild-type protein. This result confirms that the neutralization of the transient hydronium ion by the negative charge of β-Glu 188 facilitates the formation of the nucleophile OH^- from the catalytic water, without altering the ΔG_0 of the reaction. A second local minimum observed in the top right-hand corner of Figure 5 suggests that, in the absence of the β-Glu 188 residue, a direct proton transfer from the catalytic water molecule to the nucleotide appears to be the most favorable pathway. However, this alternative proton transfer path must proceed through an energy barrier of ∼32 kcal/mol, notably higher than the value of 22 kcal/mol obtained for the sequential transfer of the proton involving the two water molecules in the wild-type protein.

Recently, experimental data based on single-molecule observations[25] have provided evidence that the rate-determining step of the reaction is the transfer of a proton from the catalytic water, a statement that completely agrees with our results. In the same work, additional experimental results were interpreted as being favorable to a "dissociative" reaction path in which the $P\gamma-O_\beta$ bond of ATP was weakened before the proton transfer event in a "nonconventional" S_N1 process, although the authors do not discard the possibility that both processes, the rate-determining step of proton transfer and the weakening of the $P_\gamma-O_\beta$ bond, can occur in a concerted manner.

In summary, our results are compatible with a mechanism for catalytic water activation of F_1-ATPase involving two water molecules and the transfer of a proton from the catalytic water (wat A) to a second water (wat B) and then to the ATP molecule that acts as the proton acceptor. The important role of β-Glu 188 is the stabilization of the transient water structures during the proton transfer. This mechanism has been described using a new approach for energy surface calculations of QM/MM trajectories, allowing a detailed analysis of the conformational space defined by the reaction coordinates. Previous results obtained using the same methodology for human Ras GTP hydrolysis[27] showed a similar mechanism involving two water molecules in the activation. Additional studies are in progress to analyze whether this mechanism could be a common solution for several GTPase and ATPase enzymes.

■ ASSOCIATED CONTENT

Supporting Information

A video demonstrating proton movements in the QM region of the QM/MM system and a figure of the simulation of proton transference between a Glu residue and an ATP molecule through a hydronium intermediate in solution. This material is available free of charge via the Internet at http://pubs.acs.org.

■ AUTHOR INFORMATION

Corresponding Author

*E-mail: pagomez@cbm.uam.es. Phone: (+34) 91 196 4663.

Author Contributions

P.G.-P. and J.M. are co-last authors.

Funding

This work was supported by Spanish Ministerio de Economía y Competitividad (MINECO) Grants SAF2007-61926, IPT2011-0964-900000, and SAF2011-13156-E and by the European Commission through Grants FP7 HEALTH-F3-2009-223431 (EU Project "Divinocell") and FP7 HEALTH-2011-278603 (EU Project "Dorian"). Work at Biomol-Informatics was partially financed by the European Social Fund.

Notes

The authors declare no competing financial interest.

■ ACKNOWLEDGMENTS

We thank Toffa Evans for valuable assistance with the manuscript. We also thank the "Fundación Ramón Areces", and the computational support of the "Centro de Computación Científica CCC-UAM" is acknowledged.

■ REFERENCES

(1) Boyer, P. D. (1997) The ATP synthase: A splendid molecular machine. *Annu. Rev. Biochem. 66*, 717−749.

(2) Senior, A. E., Nadanaciva, S., and Weber, J. (2002) The molecular mechanism of ATP synthesis by F1F0-ATP synthase. *Biochim. Biophys. Acta 1553*, 188−211.

(3) Alberts, B. (1998) The cell as a collection of protein machines: Preparing the next generation of molecular biologists. *Cell 92*, 291−294.

(4) Karplus, M., and Pu, J. (2010) How Biomolecular Motors Work: Synergy Between Single Molecule Experiments and Single Molecule Simulations. In *Single Molecule Spectroscopy in Chemistry, Physics and Biology* (Gräslund, A., Rigler, R., and Widengren, J., Eds.) pp 3−22, Springer, Berlin.

(5) Karplus, M., and Gao, Y. Q. (2004) Biomolecular motors: The F1-ATPase paradigm. *Curr. Opin. Struct. Biol. 14*, 250−259.

(6) Nakamoto, R. K., Ketchum, C. J., Kuo, P. H., Peskova, Y. B., and Al-Shawi, M. K. (2000) Molecular mechanisms of rotational catalysis in the F_0F_1 ATP synthase. *Biochim. Biophys. Acta 1458*, 289−299.

(7) Gao, Y. Q., Yang, W., and Karplus, M. (2005) A structure-based model for the synthesis and hydrolysis of ATP by F1-ATPase. *Cell 123*, 195−205.

(8) Abrahams, J. P., Leslie, A. G., Lutter, R., and Walker, J. E. (1994) Structure at 2.8 Å resolution of F1-ATPase from bovine heart mitochondria. *Nature 370*, 621−628.

(9) Braig, K., Menz, R. I., Montgomery, M. G., Leslie, A. G., and Walker, J. E. (2000) Structure of bovine mitochondrial F_1-ATPase inhibited by Mg^{2+}ADP and aluminium fluoride. *Structure 8*, 567−573.

(10) Gibbons, C., Montgomery, M. G., Leslie, A. G., and Walker, J. E. (2000) The structure of the central stalk in bovine F_1-ATPase at 2.4 Å resolution. *Nat. Struct. Biol. 7*, 1055−1061.

(11) Kagawa, R., Montgomery, M. G., Braig, K., Leslie, A. G., and Walker, J. E. (2004) The structure of bovine F1-ATPase inhibited by ADP and beryllium fluoride. *EMBO J. 23*, 2734−2744.

(12) Menz, R. I., Walker, J. E., and Leslie, A. G. (2001) Structure of bovine mitochondrial F_1-ATPase with nucleotide bound to all three catalytic sites: Implications for the mechanism of rotary catalysis. *Cell 106*, 331−341.

(13) Itoh, H., Takahashi, A., Adachi, K., Noji, H., Yasuda, R., Yoshida, M., and Kinosita, K. (2004) Mechanically driven ATP synthesis by F1-ATPase. *Nature 427*, 465−468.

(14) Rees, D. M., Montgomery, M. G., Leslie, A. G., and Walker, J. E. (2012) Structural evidence of a new catalytic intermediate in the

pathway of ATP hydrolysis by F1-ATPase from bovine heart mitochondria. *Proc. Natl. Acad. Sci. U.S.A. 109*, 11139−11143.
(15) Yang, Y., and Cui, Q. (2009) Does water relay play an important role in phosphoryl transfer reactions? Insights from theoretical study of a model reaction in water and tert-butanol. *J. Phys. Chem. B 113*, 4930−4939.
(16) Lahiri, S. D., Zhang, G., Dunaway-Mariano, D., and Allen, K. N. (2003) The pentacovalent phosphorus intermediate of a phosphoryl transfer reaction. *Science 299*, 2067−2071.
(17) Cleland, W. W., and Hengge, A. C. (2006) Enzymatic mechanisms of phosphate and sulfate transfer. *Chem. Rev. 106*, 3252−3278.
(18) Bianchet, M. A., Hullihen, J., Pedersen, P. L., and Amzel, L. M. (1998) The 2.8-Å structure of rat liver F1-ATPase: Configuration of a critical intermediate in ATP synthesis/hydrolysis. *Proc. Natl. Acad. Sci. U.S.A. 95*, 11065−11070.
(19) Tozawa, K., Ohbuchi, H., Yagi, H., Amano, T., Matsui, T., Yoshida, M., and Akutsu, H. (1996) Unusual pKa of the carboxylate at the putative catalytic position of the thermophilic F1-ATPase β subunit determined by ^{13}C-NMR. *FEBS Lett. 397*, 122−126.
(20) Kaczmarek, P., Szczepanik, W., and Jezowska-Bojczuk, M. (2005) Acid-base, coordination and oxidative properties of systems containing ATP, L-histidine and Ni(II) ions. *Dalton Trans.*, 3653−3657.
(21) Schweins, T., Langen, R., and Warshel, A. (1994) Why have mutagenesis studies not located the general base in ras p21. *Nat. Struct. Biol. 1*, 476−484.
(22) Schweins, T., Geyer, M., Scheffzek, K., Warshel, A., Kalbitzer, H. R., and Wittinghofer, A. (1995) Substrate-assisted catalysis as a mechanism for GTP hydrolysis of p21ras and other GTP-binding proteins. *Nat. Struct. Biol. 2*, 36−44.
(23) Dittrich, M., Hayashi, S., and Schulten, K. (2003) On the mechanism of ATP hydrolysis in F1-ATPase. *Biophys. J. 85*, 2253−2266.
(24) Dittrich, M., Hayashi, S., and Schulten, K. (2004) ATP hydrolysis in the βTP and βDP catalytic sites of F1-ATPase. *Biophys. J. 87*, 2954−2967.
(25) Hayashi, S., Ueno, H., Shaikh, A. R., Umemura, M., Kamiya, M., Ito, Y., Ikeguchi, M., Komoriya, Y., Iino, R., and Noji, H. (2012) Molecular Mechanism of ATP Hydrolysis in F_1-ATPase Revealed by Molecular Simulations and Single-Molecule Observations. *J. Am. Chem. Soc. 134*, 8447−8454.
(26) Onishi, H., Mochizuki, N., and Morales, M. F. (2004) On the myosin catalysis of ATP hydrolysis. *Biochemistry 43*, 3757−3763.
(27) Martin-Garcia, F., Mendieta-Moreno, J. I., Lopez-Vinas, E., Gomez-Puertas, P., and Mendieta, J. (2012) The Role of Gln61 in HRas GTP hydrolysis: A quantum mechanics/molecular mechanics study. *Biophys. J. 102*, 152−157.
(28) Case, D. A., Darden, T. A., Cheatham, T. E., III, Simmerling, C. L., Wang, J., Duke, R. E., Luo, R., Walker, R. C., Zhang, W., Merz, K. M., Roberts, B., Wang, B., Hayik, S., Roitberg, A., Seabra, G., Kolossvai, I., Wong, K. F., Paesani, F., Vanicek, J., Liu, J., Wu, X., Brozell, S. R., Steinbrecher, T., Gohlke, H., Cai, Q., Ye, X., Wang, J., Hsieh, M.-J., Cui, G., Roe, D. R., Mathews, D. H., Seetin, M. G., Sagui, C., Babin, V., Luchko, T., Gusarov, S., Kovalenko, A., and Kollman, P. A. (2010) *Amber 11 User's Manual* (http://www.ambermd.org).
(29) Walker, R. C., Crowley, M. F., and Case, D. A. (2008) The implementation of a fast and accurate QM/MM potential method in Amber. *J. Comput. Chem. 29*, 1019−1031.
(30) Babin, V., Roland, C., and Sagui, C. (2008) Adaptively biased molecular dynamics for free energy calculations. *J. Chem. Phys. 128*, 134101.
(31) Park, S., Khalili-Araghi, F., Tajkhorshid, E., and Schulten, K. (2003) Free energy calculation from steered molecular dynamics simulations using Jarzynski's equality. *J. Chem. Phys. 119*, 3559−3566.
(32) Kastner, J., and Thiel, W. (2005) Bridging the gap between thermodynamic integration and umbrella sampling provides a novel analysis method: "Umbrella integration". *J. Chem. Phys. 123*, 144104.
(33) Cukierman, S. (2006) Et tu, Grotthuss! and other unfinished stories. *Biochim. Biophys. Acta 1757*, 876−885.
(34) Nathanson, L., and Gromet-Elhanan, Z. (2000) Mutations in the β-subunit Thr(159) and Glu(184) of the *Rhodospirillum rubrum* F_0F_1 ATP synthase reveal differences in ligands for the coupled Mg^{2+}- and decoupled Ca^{2+}-dependent F_0F_1 activities. *J. Biol. Chem. 275*, 901−905.
(35) Enoki, S., Watanabe, R., Iino, R., and Noji, H. (2009) Single-molecule study on the temperature-sensitive reaction of F1-ATPase with a hybrid F1 carrying a single β(E190D). *J. Biol. Chem. 284*, 23169−23176.
(36) Amano, T., Tozawa, K., Yoshida, M., and Murakami, H. (1994) Spatial precision of a catalytic carboxylate of F1-ATPase β subunit probed by introducing different carboxylate-containing side chains. *FEBS Lett. 348*, 93−98.
(37) Nathanson, L., and Gromet-Elhanan, Z. (1998) Mutagenesis of β-Glu-195 of the *Rhodospirillum rubrum* F1-ATPase and its role in divalent cation-dependent catalysis. *J. Biol. Chem. 273*, 10933−10938.